

ASSOCIATION PHENOMENA AND ENHANCEMENT OF LIGHT-INDUCED CHARGE SEPARATION IN THE Ru[(C₁₃H₂₇)₂bpy]₃²⁺-METHYL VIOLOGEN SYSTEM (bpy ≡ 2,2'-BIPYRIDYL) IN LARGE SODIUM DODECYLSULPHATE MICELLES†

F. STEINMÜLLER and H. RAU

Fachgebiet Physikalische Chemie, Institut für Chemie, Universität Hohenheim, D-7000 Stuttgart 70 (F.R.G.)

(Received January 3, 1985; in revised form February 22, 1985)

Summary

The highly hydrophobic complex tris-(4,4'-di-tridecyl-2,2'-bipyridyl)-Ru^{II} associates in rod-like sodium dodecylsulphate (SDS) micelles formed at high ionic strength. The associate emits at 670 nm with $\tau = 300$ ns and a quantum yield of about 1% (the monomer emits at 608 nm with $\tau \approx 1150$ ns and a quantum yield of 5% - 10%). Association is not observed in concentrated homogeneous solutions in organic solvents. Concomitant with the association of the complex an enhancement of light-induced charge separation in the Ru[(C₁₃H₂₇)₂bpy]₃²⁺-MV²⁺-edta-SDS system (bpy ≡ 2,2'-bipyridyl; MV²⁺ ≡ methyl viologen; edta ≡ ethylenediaminetetraacetic acid) is observed in rod-like micelles.

1. Introduction

Phase boundaries are widely used, particularly in micellar systems, in work aimed at attaining persistent light-induced charge separation [1]. The surface charges on micelles support the separation of the charged products of the primary light-induced electron transfer process. Negative surface charges, such as those on sodium dodecylsulphate (SDS) micelles, favour charge separation when an electron is transferred from an excited donor species in the micelle to an acceptor species in the water phase. We have used a modification of the well-known "sacrificial" system Ru(bpy)₃²⁺-MV²⁺-edta (bpy ≡ 2,2'-bipyridyl; MV²⁺ ≡ methyl viologen; edta ≡ ethylenediaminetetraacetic acid) in which the bpy ligands have been substituted with hydrocarbon chains of various lengths. We report on the new complex

†Dedicated to Professor Dr. Dietrich Schulte-Frohlinde on the occasion of his 60th birthday.

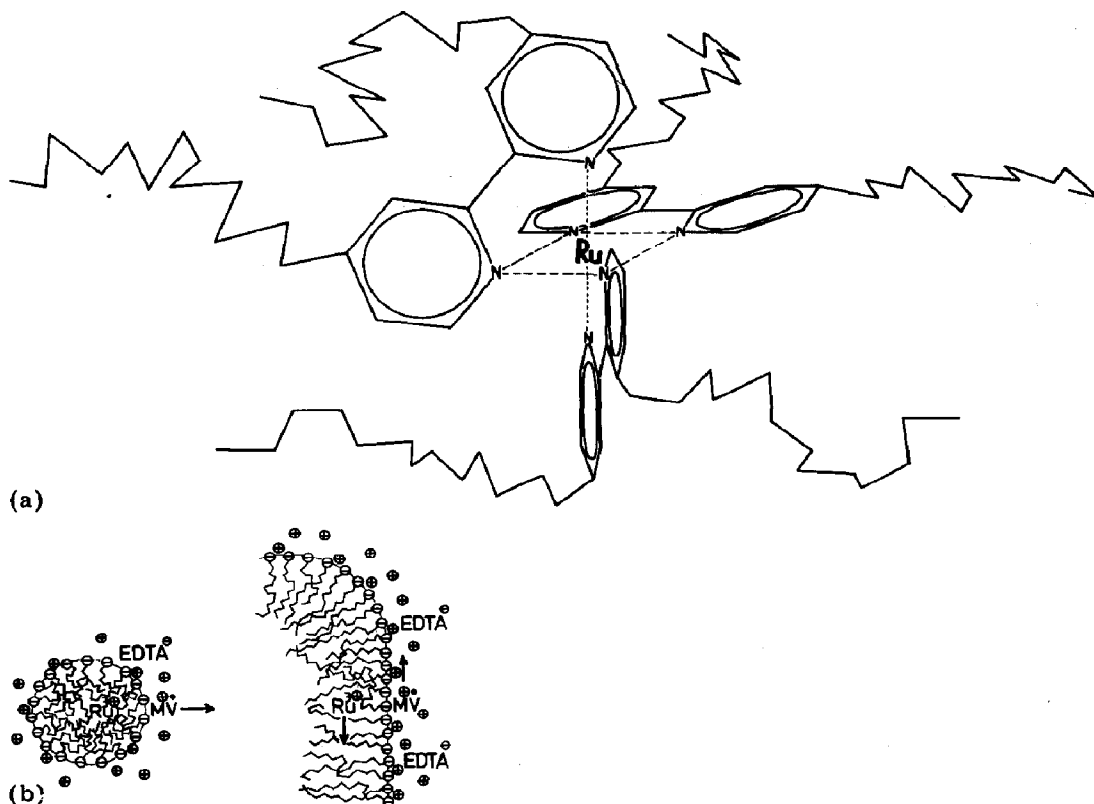


Fig. 1. (a) Structure of the $\text{Ru}[(\text{C}_{13}\text{H}_{27})_2\text{bpy}]_3^{2+}$ ion; (b) the reacting species in small spherical and large rod-like micelles.

$\text{Ru}[4,4'-(\text{C}_{13}\text{H}_{27})_2\text{bpy}]_3\text{Cl}_2$ (Fig. 1(a)) as a representative of the sequence of C_7 , C_{11} - and C_{13} -substituted complexes. This compound is completely insoluble in water and resides within the SDS micelle (this system thus differs from the annelide system of ref. 2).

In normal spherical micelles charge separation requires the diffusion of the primary electron transfer product $\text{MV}^{\cdot+}$ away from the boundary as the micelle is too small for the donor to move away. In large micelles both the acceptor and the donor have a fair chance of diffusing apart within the region of the boundary and this lateral diffusion may favour charge separation (Fig. 1(b)).

In this paper we report the effect of a change of the SDS micelles on the sacrificial charge-separation system described above. We observe an increase in $\text{MV}^{\cdot+}$ radical production when we induce the transition to large rod-like micelles by increasing the ionic strength of the solution. The principle of lateral diffusion has also been tested in phosphatidylcholine vesicles, but we could not detect any light-induced charge separation [3].

Unexpectedly the rod-like SDS micelles favour an association of ruthenium trisbipyridyl complexes substituted with hydrocarbon chains

containing seven or more carbon atoms. This association leads to a spectroscopically well-defined species, probably a dimer, which cannot be induced by high complex concentration in homogeneous solution in organic solvents.

2. Experimental details

2.1. Materials

The synthesis of ruthenium complexes substituted by six hydrocarbon chains (CH_3 , C_5H_{11} , C_7H_{15} , $\text{C}_{11}\text{H}_{23}$ and $\text{C}_{13}\text{H}_{27}$) is reported elsewhere [4]. $\text{Ru}[(\text{bpy})_3]\text{Cl}_2$ (EGA), methyl viologen (EGA, Fluka) and edta (Merck, Fluka) were used as received (all were pro analysis grade). Triethanolamine (Merck) was redistilled before use. *n*-Hexane and trichloromethane were Merck Uvasol grade. Water was distilled twice from a quartz apparatus and ethanol was distilled in a rectifying column to spectroscopic grade. SDS (Merck) was extracted for 72 h with spectroscopic grade *n*-hexane in a Soxhlet apparatus, cholesterol (Merck) was recrystallized, and phosphatidylcholine (10% in trichloromethane) (Sigma) and sodium cholate (Merck) were used as received.

2.2. Preparation of the microheterogeneous systems

Vesicles were prepared from phosphatidylcholine–cholate–cholesterol solutions by sonification, ether evaporation and dialysis. Micellar solutions of SDS were prepared by stirring or shaking solid SDS and water or dilute SDS solutions. $\text{Ru}[(\text{C}_{13}\text{H}_{27})_2\text{bpy}]_3\text{Cl}_2$ is completely insoluble in water, so that it was necessary to dissolve the complex in *n*-hexane in order to prepare an emulsion with the SDS solution by sonification. The *n*-hexane was removed under vacuum. The complex concentrations quoted in this paper are overall concentrations as determined spectroscopically with the assumption of identical ϵ values for ethanol (EtOH) and SDS micelles. The SDS content was increased by adding solid SDS to the solutions containing the complex in micelles. The critical micelle concentration (CMC) of the complex-loaded micelles was approached from the high concentration side. Conductivity measurements were made using WTW (Wiss.-Techn. Werkstätten, 812 Weilheim, F.R.G.) apparatus. The pH was determined with a glass electrode; when no buffers were used adjustments were made by adding NaOH (Suprapur grade) until the desired value was attained.

2.3. Preparation of the samples

All solutions for emission lifetime and intensity measurements and for electron transfer experiments were oxygen free at 300 K. Deoxygenation was carried out by passing an argon stream over the surfaces of the solutions, which were contained in rectangular spectrometric cells, for at least 4 h (usually overnight). Problems involving foaming were encountered with the freeze–pump–thaw method, and it was only used to establish the efficiency of the argon flushing procedure. After deoxygenation the cells

were closed either by a stopcock or by sealing. We were unable to achieve complete reproducibility of the results in the preparation of the micellar samples.

2.4. Spectroscopy

The absorption and emission spectra were obtained using a Zeiss DMR 10 spectrometer and a Farrand spectrometer respectively. The emission lifetimes were determined by flashing the samples with the 337 nm line of a Lambda Physik EMG 500 excimer laser operated with nitrogen. The signal was detected using an Oriel double monochromator, an RCA C 31034 A photomultiplier with a Knott SKD emitter-follower and a Tektronix 7834 storage oscilloscope. The polaroid traces were analysed on a Tektronix 4052 computer using a curve-fitting program written by R. Frank. The emission spectra were corrected, when necessary, by comparison with an *N,N*-dimethylamino-2-nitrobenzene standard [5].

2.5. Photochemistry

The irradiations were performed at room temperature in either fused or stopcocked cells using a Schott KL 1500 cold light source which is a visible light source similar to a broad band projector lamp. The solutions were stirred with a magnetic bar. The photoreaction yield was determined using a four-step procedure.

(a) The intensity I_0 (in einsteins per second per square metre) (ref. 6, p. 287) impinging on a rectangular spectrophotometric cell in an arrangement consisting of a Philips HPK 125 W mercury lamp and a 436 nm Schott UV PIL filter was determined using Parker's ferrous oxalate actinometer.

(b) The actinometric cell was replaced by a cell filled with a solution containing 0.2 M edta, 3×10^{-3} M MV^{2+} and 2×10^{-5} M $Ru[(C_{13}H_{27})_2\text{-bpy}]_3Cl_2$ in EtOH. The apparent integral quantum yield QY of product formation (ref. 6, p. 134) was computed from the results of five runs using the expression

$$QY = \frac{c_{MV^{2+}}}{t \times 10^3 (1 - 10^{-E'}) I_0}$$

where E' is the absorbance at 436 nm which is almost independent of time as the developing MV^{2+} contributes very little.

(c) Four solutions of the same composition as that used in (b) were irradiated with the broad band cold light source and the apparent absorbed intensity per second $(1 - 10^{-E'}) I_0$ was calculated using the yield determined in (b).

(d) A solution containing the same concentrations of the complex, MV^{2+} and edta in a 10^{-2} M SDS micellar solution was irradiated with the cold light source. Six runs were performed. The apparent absorbed intensity from (c) was used to calculate the apparent integral quantum yield of production of MV^{2+} . This is a good approximation as the absorption spectra of the ruthenium complex in SDS and EtOH have the same shape and a relative

displacement of as little as 10 nm. We obtained a yield of 5×10^{-4} which is an order-of-magnitude figure.

3. Results

3.1. Characterization of the micellar system

The first critical micelle concentration (CMC I) for SDS in water was determined by conductivity measurements and was found to be $(7.9 \pm 1.0) \times 10^{-3}$ M in agreement with the literature [7]. Incorporation of $\text{Ru}[(\text{C}_{13}\text{H}_{27})_2\text{bpy}]_3\text{Cl}_2$ did not change the CMC I of the micellar solution $((8.7 \pm 1.0) \times 10^{-3}$ M). It is well known that higher ionic strength induces growth of the SDS micelles to form large spherical aggregates [8]. The CMC I of SDS in 0.2 M edta solution was determined by using the change in the lifetime of (unsubstituted) $\text{Ru}(\text{bpy})_3^{2+}$ upon micelle formation [9] and was found to be $(3.5 \pm 0.8) \times 10^{-4}$ M. In view of the similarity in formation of micelles containing $\text{Ru}[(\text{C}_{13}\text{H}_{27})_2\text{bpy}]_3^{2+}$ and empty micelles (see above) we assumed the same CMC I for micelles loaded with the hydrophobic complex in 0.2 M edta.

The addition of SDS to concentrations beyond CMC I has the same effect as increasing the ionic strength: the aggregation number increases [10] and large spherical micelles are formed.

Higher concentrations of SDS at high salt concentrations lead to a transition of the large spherical micelles to large rod-like micelles at a second critical concentration (CMC II) which, however, seems not to be as sharply defined as CMC I [10, 11]. We used a very simple indicator, *i.e.* light scattering measured as absorption in the spectrophotometer, to determine CMC II. For example, a plot of the apparent A_{330} versus c_{SDS} at pH 7 with 0.2 M edta showed a discontinuity at 0.15 M SDS. Ikeda and coworkers [12] have found that the sphere-rod transition occurs in this concentration range ($c_{\text{SDS}} + c_{\text{salt}} = 0.4$ M). Our electron transfer data (see below) also indicate the occurrence of a structural change at this ionic strength.

In summary we have to separate three types of micelle in this work: small spherical micelles at low ionic strength, large spherical micelles at high ionic strength and low SDS concentration, and large rod-like micelles at high ionic strength and high SDS concentration.

3.2. The ruthenium-bipyridyl complexes

$\text{Ru}(\text{bpy})_3^{2+}$ is water soluble and is known to accumulate in the Stern layer of micelles bearing negative surface charges [1]. The methyl-substituted complex shows similar behaviour. The solubility in water decreases with increasing length of the hydrocarbon substituents, and the C_{11} and C_{13} species are so insoluble in water that special techniques (see Section 2) are necessary to solubilize them into the micelles where they almost certainly reside in the hydrocarbon core.

3.3. Absorption and emission

The absorption spectra of all alkyl-substituted $\text{Ru}(\text{bpy})_3^{2+}$ complexes with C_1 , C_5 , C_7 , C_{11} and C_{13} chains in EtOH are similar to those of $\text{Ru}(\text{bpy})_3^{2+}$ ($\lambda_{\text{max}} = 450 \text{ nm}$) but are red shifted by 10 nm. In spherical SDS micelles the lowest energy absorption band of the long-chain substituted complexes shows distinct structure. When 0.2 M edta is added and the SDS concentration is increased the absorption spectrum changes (Fig. 2). An isosbestic point seems to develop at 490 nm. Light scattering can never be completely avoided in micellar solutions and Mauser A diagrams (ref. 6, Chapter 4, and ref. 13) are not very informative either as the errors of ΔA in the slopes are appreciable. On this basis we cannot claim a uniform reaction but undoubtedly the absorption spectra indicate the presence of a new absorbing species. The emission spectra of $\text{Ru}(\text{bpy})_3^{2+}$ ($\lambda_{\text{max}} = 640 \text{ nm}$) and $\text{Ru}[(\text{CH}_3)_2\text{bpy}]_3^{2+}$ ($\lambda_{\text{max}} = 650 \text{ nm}$) in solutions with low SDS concentrations (small and large spherical micelles) are red shifted relative to their spectral position in EtOH ($\lambda_{\text{max}} = 610 \text{ nm}$) [14]. $\text{Ru}[(\text{C}_{13}\text{H}_{27})_2\text{bpy}]_3^{2+}$ does not show such a shift ($\lambda_{\text{max}} = 608 \text{ nm}$). The spectral shift of the emission band in the complex series can be correlated with the hydrophobicity of the complex.

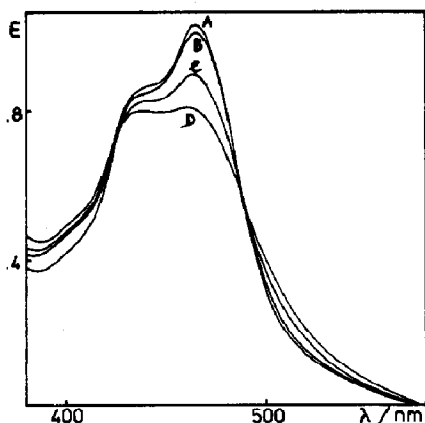


Fig. 2. Absorption spectrum of $4.5 \times 10^{-5} \text{ M Ru}[(\text{C}_{13}\text{H}_{27})_2\text{bpy}]_3^{2+}$ in the presence of $10^{-3} \text{ M MV}^{2+}$, 0.2 M edta (pH 8.8) and various SDS concentrations: curve A, 0.02 M; curve B, 0.043 M; curve C, 0.110 M; curve D, 0.172 M.

High SDS concentrations (large rod-like micelles) result in a new emission spectrum for the water-insoluble complexes but not, however, for the water-soluble complexes. Figure 3 shows the uncorrected emission spectrum of $\text{Ru}[(\text{C}_{13}\text{H}_{27})_2\text{bpy}]_3^{2+}$ on excitation at $\lambda = 460 \text{ nm}$ and the excitation spectra for $\lambda_{\text{em}} = 600 \text{ nm}$ and $\lambda_{\text{em}} = 670 \text{ nm}$ in 0.31 M SDS (+0.2 M edta). The emission spectrum shows two bands. The short-wavelength contour fits the contour of the emission spectrum in EtOH which is included in Fig. 3. The emission band at low energy is obtained by subtracting the EtOH spectrum from the SDS spectrum. The emission excitation spectrum indicates

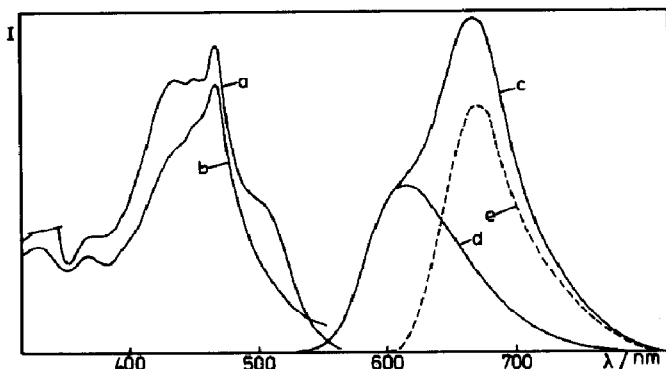


Fig. 3. Uncorrected excitation and emission spectra of $\text{Ru}[(\text{C}_{13}\text{H}_{27})_2\text{bpy}]_3^{2+}$ in 0.32 M SDS + 0.2 M edta: curve a, excitation spectrum ($\lambda_{\text{em}} = 680$ nm); curve b, excitation spectrum ($\lambda_{\text{em}} = 580$ nm); curve c, emission spectrum ($\lambda_{\text{exc}} = 460$ nm); curve d, emission spectrum of the monomer in EtOH; curve e, emission spectrum of the dimer obtained by subtracting curve d from curve c.

a superposition of the absorptions of the species emitting at 608 nm and at 670 nm. The excitation spectrum is in accordance with the absorption spectrum: increased absorption is observed on both sides of the main absorption band of the species emitting at 608 nm. The emission characteristics undergo a continuous transition rather than an abrupt change at a critical SDS concentration. The emission spectra obtained at various SDS concentrations can be used to construct a plot of I_{660} versus I_{600} [15] which is linear and indicates that the emitting species undergoes a uniform reaction. This implies association of the complex to form dimers.

The favourable forms of the two emission bands allow resolution of the band contour (see Fig. 3). Therefore we can estimate the degree of association by comparing the integrated intensity of the resolved 608 nm band in, for example, 0.31 M SDS + 0.2 M edta with that of the simple 608 nm band in 0.01 M SDS + 0.2 M edta for the same concentration of $\text{Ru}[(\text{C}_{13}\text{H}_{27})_2\text{bpy}]_3^{2+}$. On assuming a constant emission quantum yield of the monomeric complex in both solutions we find a reduction of the monomer concentration to 5% which means that the monomer-to-dimer ratio is 1:10.

The decay dynamics of the C_{13} complex in micellar solutions containing 0.2 M edta can be approximated by biexponential kinetics. At low SDS concentrations (large spherical micelles) the two lifetimes are about 1150 ± 100 ns and 300 ± 80 ns. They can be attributed to the species emitting at 608 nm and 670 nm respectively. The dependence on SDS concentration is indicated in Fig. 4 where the decay curve analysis at 600 nm is presented in terms of lifetimes (Fig. 4(a)) and relative weights (pre-exponential factors) (Fig. 4(b)). At high SDS concentrations (large rod-like micelles) the decay is single exponential. Figure 4 indicates that a change in the decay characteristics occurs near 0.15 M SDS.

The emission quantum yields of $\text{Ru}[(\text{C}_{13}\text{H}_{27})_2\text{bpy}]_3^{2+}$ in homogeneous EtOH and heterogeneous solutions were determined using $\text{Ru}(\text{bpy})_3^{2+}$ in

water as a reference ($\phi = 0.041$) [16]. Application of the equation

$$\frac{\phi_x}{\phi_{\text{ref}}} = \left(\frac{n_x}{n_{\text{ref}}} \right)^2 \frac{I_x}{I_{\text{ref}}} \frac{1 - 10^{-E'_{\text{ref}}}}{1 - 10^{-E'_x}}$$

gave $\phi_{\text{EtOH}}^{\text{mono}} = 0.065 \pm 15\%$ (leading to $\tau_0 = 0.810/0.065 \mu\text{s} \approx 12 \mu\text{s}$) and $\phi_{\text{SDS}}^{\text{mono}} = 0.085$. We cannot give an error margin for $\phi_{\text{SDS}}^{\text{mono}}$ because no data are available for the refractive index n (we have assumed $n_{\text{SDS}}/n_{\text{H}_2\text{O}} = 1$). The order of magnitude of $\tau_{\text{SDS}}^{\text{mono}}$ is corroborated by relating the measured lifetime τ to τ_0 : $\phi_{\text{SDS}}^{\text{mono}} = 1.2 \mu\text{s}/12 \mu\text{s} = 0.10$. The following procedure was used to estimate $\phi_{\text{SDS}}^{\text{dim}}$. The absorption of the dimer at the excitation wavelength of 450 nm is the total absorbance minus the absorbance of the remaining monomer which is known to be 5% of the monomer absorbance in the 0.01 M SDS solution (see above). The total complex concentration was held constant. The corrected integrated emission intensities I_x and I_{ref} are rather uncertain because the photomultiplier sensitivity varies markedly in this wavelength range. Thus we cannot give more than a very crude estimate of the dimer emission yield which is of the order of 1%.

3.4. Electron transfer

Electron transfer is indicated by the quenching of the emission of $\text{Ru}[(\text{C}_{13}\text{H}_{27})_2\text{bpy}]_3^{2+}$ and the creation of the blue $\text{MV}^{\cdot+}$ radical cation.

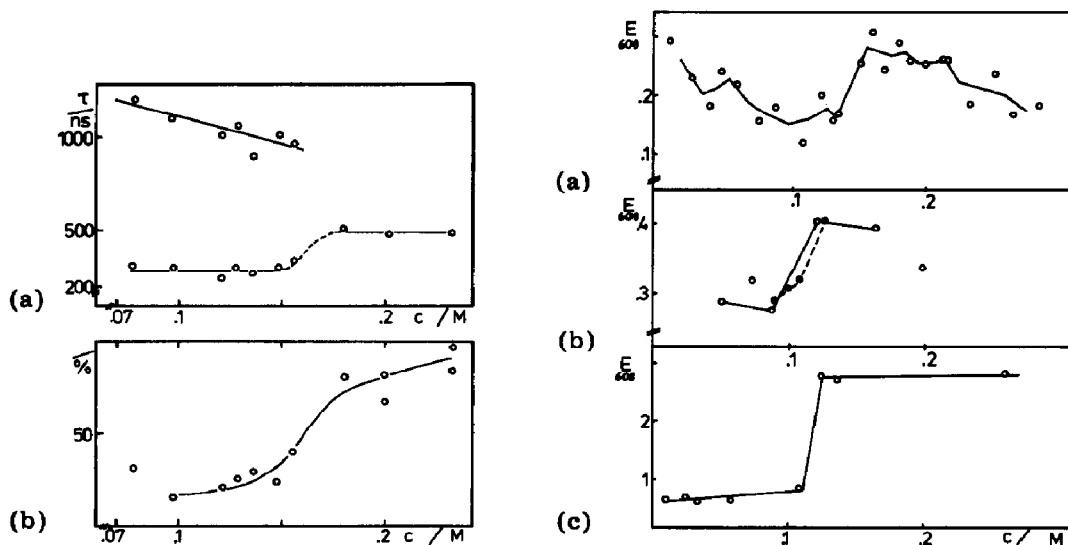


Fig. 4. Decay times of $\text{Ru}[(\text{C}_{13}\text{H}_{27})_2\text{bpy}]_3^{2+}$ in an SDS solution (pH 8.8) containing 10^{-3} M MV^{2+} and 0.2 M edta: (a) lifetimes; (b) pre-exponential factors.

Fig. 5. Production of the $\text{MV}^{\cdot+}$ radical in SDS solutions: (a) 0.2 M edta, 5.8×10^{-5} M $\text{Ru}[(\text{C}_{13}\text{H}_{27})_2\text{bpy}]_3^{2+}$ (pH 8.6) and 3×10^{-3} M MV^{2+} ; (b) 0.2 M edta, 5.8×10^{-5} M $\text{Ru}[(\text{C}_{13}\text{H}_{27})_2\text{bpy}]_3^{2+}$ (pH 9.75) and 3×10^{-3} M MV^{2+} ; (c) 0.25 M edta, 8.3×10^{-6} M $\text{Ru}[(\text{C}_{13}\text{H}_{27})_2\text{bpy}]_3^{2+}$ (pH 10 - 11) and 10^{-3} M MV^{2+} .

Stern-Volmer plots of stationary quenching experiments performed in 0.01 M SDS solutions containing no edta (small spherical micelles) and up to 1.7×10^{-3} M MV^{2+} give a quenching constant k_q of $1.0 \times 10^9 \text{ dm}^3 \text{ mol}^{-1} \text{ s}^{-1}$. Quenching experiments in 0.01 M SDS containing 0.2 M edta (large spherical micelles) and up to 2.5×10^{-2} M MV^{2+} gave a quenching constant $k_{q,608}$ of $(5 \pm 1.5) \times 10^6 \text{ dm}^3 \text{ mol}^{-1} \text{ s}^{-1}$ for the monomeric species emitting at 608 nm. In 0.31 M SDS containing 0.2 M edta (large rod-like micelles) and up to 4×10^{-2} M MV^{2+} the quenching of the dimer emission is about a factor of 5 higher ($k_{q,670} = (3.2 \pm 1.5) \times 10^7 \text{ dm}^3 \text{ mol}^{-1} \text{ s}^{-1}$).

The quenching of the emission of the complex residing in the micellar core by MV^{2+} in the water phase (Fig. 1(b)) is not accompanied by a persistent $MV^{\cdot+}$ concentration unless edta is present. We have to assume the usual thermal back electron transfer across the phase boundary. If, however, edta is added it dissolves in the water phase and a persistent colour characteristic of $MV^{\cdot+}$ is observed. Thermal back electron transfer also occurs across the phase boundary from edta as a donor which is present in high concentrations (10^{-2} M). When triethanolamine is added to the system it partitions between the micellar core and the water phase and back electron transfer occurs within the micelle. The production of $MV^{\cdot+}$ then increases by a factor of 6 - 8.

The $MV^{\cdot+}$ yield at constant irradiation times is shown as a function of the SDS concentration in Fig. 5. Two features should be noted: there is a discontinuity in $MV^{\cdot+}$ production between 0.12 and 0.18 M SDS and $MV^{\cdot+}$ production is favoured by higher pH. We used the four-step procedure outlined in Section 2 to obtain an estimate of the order of magnitude of the reaction yield of $MV^{\cdot+}$ radicals. We found a yield of 10^{-4} - 10^{-3} for the system with large spherical micelles (low SDS concentration).

4. Discussion

A problem in the interpretation of light-induced electron transfer from a donor in a micellar aggregate to an acceptor in the continuous water phase is the uncertainty in the positions and local environments of the participating species. By observing the properties of a series of C_nH_{2n+1} -hexasubstituted $Ru(R_2bpy)_3^{2+}$ complexes we have ascertained that $Ru[(C_{13}H_{27})_2bpy]_3Cl_2$ resides in the inner part of the micelle and avoids polar areas. This conclusion is supported by the marked reduction of the efficiency of quenching of the complex by MV^{2+} in large micelles compared with that in small micelles. The fact that emission quenching by MV^{2+} as well as persistent $MV^{\cdot+}$ concentrations in the presence of edta as a sacrificial electron donor are observed in large structures indicates that electron transfer takes place over considerable distances and across a charged surface layer. If we estimate the thickness of the hydrocarbon sheath to be about 0.8 nm (deduced from the influence of the chain length on light-induced electron transfer in a homogeneous solution [4]) and assume the Stern layer to be of the order of, say,

0.2 nm [1], a transfer distance from centre to centre of about 1.5 - 2 nm is not unreasonable. Transfer distances of this order of magnitude have recently been observed for light-induced [17] and dark [18] reactions. The low yield of persistent $MV^{\cdot+}$ is indicative of the double electron transfer in the sacrificial system. The radical yield is increased upon addition of triethanolamine which enables the dark electron transfer to proceed in a "homogeneous" solution over a small distance.

The concentration of $Ru[(C_{13}H_{27})_2bpy]_3^{2+}$ is low enough to give a mean occupation number \bar{n} of 0.5 - 0.8 in solutions with a low SDS concentration. The addition of SDS leads to an increase in the aggregation number. The increase in micellar size is reflected by the variation of τ_{SDS}^{mono} with SDS concentration (Fig. 4(a)). Some double occupation occurs at SDS concentrations below that at which the sphere-rod transition takes place. The formation of rod-like micelles results in a marked reduction of the number of micelles present and thus the occupation number increases. Multiple occupation is frequent, and the rod-like micelles host more than one complex. It is then that we observe significant association.

An interesting feature associated with the sphere-rod transition is observed. The additional SDS molecules (which are added as solid SDS powder) could be incorporated into existing micelles and a redistribution of SDS molecules could proceed via the water phase. This would result in growth of a few micelles and dissolution of others. Thus precipitation of the water-insoluble guest molecules would be observed. Since this is not observed it is assumed that the micelles merge [19].

The association phenomenon is restricted to the large rod-like micelles. We were unable to observe it in concentrated hexane solution using front-face emission techniques. Association is almost complete in the giant micelles and the aggregates dominate the spectroscopic and photochemical properties. Several factors need to be taken into account in an assessment of the benefits of the use of giant rod-like micelles as a charge-separation system. The quenching experiments reveal that the electron transfer rate from the aggregate to MV^{2+} is increased. This effect hinders efforts to elucidate the importance of lateral diffusion for charge separation. In back electron transfer there is competition between edta and $MV^{\cdot+}$. This seems to be pH dependent as shown in Fig. 4. The redox potential on MV^{2+} is insensitive to pH changes, but it is known [20] that only the anion of edta is an efficient electron donor to $Ru(bpy)_3^{3+}$. Therefore the pH dependence may be attributable to the dissociation of edta. In conclusion, we are confronted with a complex combination of the association of the ruthenium complex, the change in the micellar structure and the dissociation of edta.

The associate which we believe to be a dimer deserves some more consideration. If we envisage interwoven hydrocarbon chains the separation of the central ruthenium ions is about 2 nm. The broadening of the absorption band and the red shift of the emission band seem to reflect a spectral pattern found in systems with exciton interaction. After electron transfer from an excited complex pair to a donor, delocalization of the remaining charge is

possible at these distances and may stabilize the initial photoproducts. There may be some parallels with polynuclear metal complexes [21]. It therefore seems worthwhile to vary the architecture of our ruthenium complexes. We plan to synthesize double $\text{Ru}(\text{bpy})_3^{2+}$ complexes linked by hydrocarbon chains of varying length. Then we shall not need the assistance of a micellar system to investigate the charge transfer properties of complex associates.

Acknowledgments

We gratefully acknowledge the support of the Deutsche Forschungsgemeinschaft and the Fonds der Chemischen Industrie, Frankfurt.

References

- 1 M. Grätzel, *Acc. Chem. Res.*, **14** (1981) 376.
N. Turro, M. Grätzel and A.-M. Braun, *Angew. Chem.*, **92** (1980) 712.
- 2 R. Knoesel, D. Markovitski, J. Simon and G. Du Portail, *J. Photochem.*, **22** (1983) 275.
- 3 S. Hidaki and F. Toda, *Chem. Lett.*, (1983) 1333.
W. E. Ford, J. W. Otvos and M. Calvin, *Nature (London)*, **274** (1978) 507; *Proc. Natl. Acad. Sci. U.S.A.*, **76** (1979) 3590.
M. Calvin, J. Willner, C. Laane and J. W. Otvos, *J. Photochem.*, **17** (1981) 195.
T. Katagi, T. Yamamura, T. Saito and S. Yukiyoishi, *Chem. Lett.*, (1981) 1451.
S. Tunuli and J. H. Fendler, *J. Am. Chem. Soc.*, **103** (1981) 2507.
L. Y.-C. Lee, J. K. Hurst, M. Politi, K. Kurihara and J. H. Fendler, *J. Am. Chem. Soc.*, **105** (1983) 370.
- 4 R. Frank, G. Greiner and H. Rau, to be published.
- 5 E. Lippert, W. Nägele, I. Seibold-Blankenstein, U. Staiger and W. Voss, *Z. Anal. Chem.*, **170** (1959) 1.
- 6 H. Mauser, *Formale Kinetik*, Bertelsmann Universitäts Verlag, Düsseldorf, 1974.
- 7 H. Mühleisen, *Dissertation*, Universität Hohenheim, 1982.
K. Shinoda, T. Nagakawa, B. Tamamushi and T. Isemura, *Some Chemical Properties of Colloidal Surfactants*, Academic Press, New York, 1963.
D. Meisel, M. S. Matheson and J. Rabani, *J. Am. Chem. Soc.*, **100** (1978) 117.
- 8 B. Lindmann and H. Wennerström, *Top. Curr. Chem.*, **87** (1980) 41.
S. Hayashi and S. Ikeda, *J. Phys. Chem.*, **84** (1980) 744.
D. J. Miller, U. K. A. Klein and H. Mauser, *Ber. Bunsenges. Phys. Chem.*, **84** (1980) 1135.
- 9 R. Frank and H. Rau, *Z. Naturforsch.*, **37a** (1982) 1253.
- 10 Y. Croonen, E. Geladé, M. van der Zegel, M. van der Auweraer, H. Vandendriessche, F. C. De Schryver and M. Almgren, *J. Phys. Chem.*, **87** (1983) 1426.
- 11 H. Hoffmann, G. Platz and W. Ulbricht, *J. Phys. Chem.*, **85** (1981) 1418.
- 12 S. Hayashi and S. Ikeda, *J. Phys. Chem.*, **84** (1980) 744.
S. Ikeda, A. Hayashi, T. Imae, *J. Phys. Chem.*, **67** (1981) 106.
- 13 H. Mauser, *Z. Naturforsch.*, **23b** (1968) 1025.
- 14 R. Frank and H. Rau, *Z. Naturforsch.*, **37a** (1982) 1253.
D. Meisel, M. A. Matheson and J. Rabani, *J. Am. Chem. Soc.*, **100** (1978) 117.
- 15 G. Gauglitz, *Z. Phys. Chem. N.F.*, **88** (1974) 193.
- 16 K. Nakamaru, K. Nishio and H. Nobe, *Sci. Rep. Hirosaki Univ.*, **26** (1979) 58.
- 17 S. Strauch, G. McLendon, M. McGuire and R. Guarr, *J. Phys. Chem.*, **87** (1983) 3579.

- E. Butty, P. Suppan and E. Haselbach, *European Postgraduate Symp. on Photochemistry, London, April 1984*.
- J. R. Miller, K. W. Hartmann and S. Abrash, *J. Am. Chem. Soc.*, **104** (1982) 4296.
- 18 J. R. Miller, J. A. Peeples, M. J. Schmitt and G. L. Closs, *J. Am. Chem. Soc.*, **104** (1982) 6488.
- 19 R. Strey and A. Pakusch, *Proc. 5th Int. Symp. on Surfactants in Solution, Bordeaux, 1984*.
- C. Tanford, Y. Nozaki and M. F. Rohde, *J. Phys. Chem.*, **81** (1977) 1555.
- 20 D. Miller and G. McLendon, *Inorg. Chem.*, **20** (1981) 950.
- 21 H. B. Gray and A. W. Maverick, *Science*, **214** (1981) 1201, and references cited therein.